Modeling Thermal Contact Resistance Between Elastic Hemisphere and Elastic Layer Bonded to Elastic Substrate

Mirko Stevanović
C-MAC Engineering Inc. (a Solectron Company)
425 Legget Drive
Kanata, Ontario, Canada K2K 2W2
Email: mstevanovic@kan.cmac.com
and
Dr. M.M. Yovanovich and Dr. J.R. Culham
University of Waterloo,
Waterloo, Ontario, Canada N2L 3G1
Email: mmyov@mhtlab.uwaterloo.ca
rix@mhtlab.uwaterloo.ca

ABSTRACT

An approximate thermo-mechanical model is developed to predict thermal contact resistance of a hemisphere in elastic contact with a layered substrate. Numerical data are obtained for several combinations of layer material. It is shown that with the proper selection of dimensionless parameters the numerical results fall on a single curve that is easily correlated. The complex solution is reduced to a simple closed form solution for the unknown contact radius. The proposed thermo-mechanical model is applicable for any layer-substrate material combination over the full range of the layer thicknesses. The agreement between the theoretical predictions and experimental data is good at the light loads. A method for correcting the contact radius for elastic-plastic behavior at higher loads is presented.

KEY WORDS: Contact radius, elastic deformation, thermal constriction resistance

NOMENCLATURE

a	contact radius, m
a_L	contact radius corresponding to layer bound, m
a_S	contact radius corresponding to substrate bound, m
a^*	dimensionless contact radius
$\bar{a}$	average contact radius, m
E	elastic modulus, Pa
F	normal load, N
F_c	critical load, N
H	hardness, Pa
n	blending parameter
k	thermal conductivity, W/mK
Q	heat transfer rate, W
R_{exp}	experimental resistance, K/W
R_j	joint resistance, K/W
R_j^*	dimensionless contact resistance
r, z	local polar coordinates
T	temperature, ^oC
t	layer thickness, m
Greek Symbols	
α	ratio of bounding radii, $\equiv a_L/a_S$
κ	conductivity ratio, $\equiv k_1/k_2$
ν	Poisson's ratio
ρ	radius of hemisphere
τ	relative layer thickness, $\equiv t/a$
ϕ	stress function
ψ	constriction parameter
Δ	difference
∇^2	Laplacian operator
Superscripts	
j	joint
*	dimensionless or reduced
Subscripts	
c	critical
e, p, ep	elastic, plastic, elastic-plastic
$e1$,$e2$	extrapolated
L, S	layer, substrate
$1, 2, 3$	layer, substrate, hemisphere

INTRODUCTION

The resistance to heat flow due to thermal spreading or constriction at a joint formed between contacts is an important consideration in the development of high speed electronic equipment. Critical interfaces formed between electronic packages or silicon flip chips and heat sinks necessitate the use of soft, compliant interface materials to fill air gaps associated with nonconforming wavy surfaces. Without the use of an interface material, the overall thermal resistance

between the heat source and the surrounding air will rise significantly, resulting in an increase in the operating temperature of the integrated circuits and a subsequent decrease in component reliability.

An example of this problem is the Thermal Conduction Module (TCM) used as an integral component of the IBM 3081 computer. Each module has an array of chips mounted on the surface. Heat generated within a single chip is removed through a spring-loaded piston, which is in contact with the chip surface as is shown in Fig. 1. The thermal resistance of the chip-piston contact controls the heat transfer rate through each cell. Using an interface material, the overall thermal resistance between the chip and piston will decrease resulting in a decrease in the operating temperature of the integrated circuits and a subsequent increase in component reliability. Sometimes the joint cannot be made permanent. Also because of the geometry of the contact, thermal greases or thin metallic foils cannot be used. In that case it is recommended to use a soft metallic or non-metallic layer as an interface material.

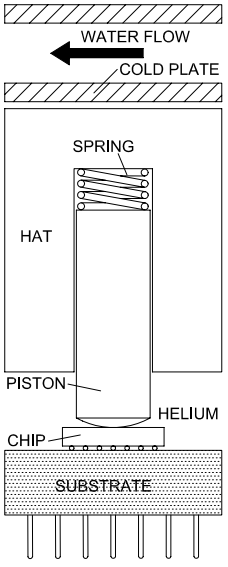

Fig.1 Basic Cell of TCM

THERMAL PROBLEM AND MODEL

The contact between a single chip, interface material and the piston is modeled as a contact between a deformable hemispherical body and a thin elastic layer, assumed to be in perfect contact with an elastic substrate of large extent. There are three pathways for the heat transfer across the contact bodies: conduction through the contact area, convection and conduction through the gap and radiation through the gap. In order to reduce the heat transfer attributed to gap conduction and convection all experiments within this study were performed in a vacuum environment. It is assumed that heat flow between contacting bodies is by conduction only through the contact area.

The temperature drop across the contact is related to the heat transfer rate and the constriction/spreading resistance, which depends on the thermal conductivities of the three components, their elastic properties (Young's modulus of elasticity and Poisson's ratio), the radius of curvature of the hemispherical body, the layer thickness and the applied mechanical load. The constriction/spreading resistance can be reduced significantly through the proper selection of the layer which has a high conductivity, low rigidity and a thickness which is sufficiently large to cause the constriction in the layer-substrate side of the joint to occur primarily within the layer.

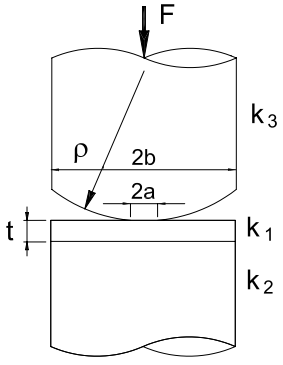

Fig.2 Model Chip - Heat Sink Contact

The layer, the substrate and the hemisphere thermal conductivities are k_1, k_2 and k_3, respectively. Since the radius of the contact area is much smaller than the radius of the hemisphere and the layered-substrate dimensions, the contact is modeled both thermally and mechanically as a circular contact connecting two half-spaces: the hemisphere on one side and the layered-substrate on the other.

The total joint resistance is defined as [1]:

$$R_j = \frac{1}{4\,a k_3} + \frac{\psi(\tau,\kappa)}{4\,a k_2} \tag{1}$$

The thermal constriction parameter $\psi(\tau,\kappa)$ is obtained from the solution of the Laplace equation within the layer and substrate together [2]. The dimensionless constriction resistance is defined with respect to the contact radius and the substrate thermal conductivity k_2:

$$R_j^* = R_j\, a\, k_2 = \frac{1}{4}\left[\frac{k_2}{k_3} + \psi(\tau,\kappa)\right] \tag{2}$$

The thermal conductivity ratio is constant for a given layer-substrate combination. The relative layer thickness varies with the mechanical load, geometry and physical properties. The evaluation of $\psi(\tau,\kappa)$ is not possible without first solving the mechanical portion of the contact resistance problem for the contact radius. The constriction/spreading resistance model will be divided into two parts: a mechanical model for solving for the unknown contact radius and a thermal model for solving the thermal portion of problem. A similar problem was investigated by Fisher [1] where he developed an approximate thermal constriction resistance model. The model requires the "transition" points

where the approximate resistance approaches the substrate and layer bounds. Fisher [1] assumed that between the two "transition" points, in the intermediate region, dimensionless resistance varies logarithmically with dimensionless layer thickness. For each material layer-substrate material combination transition points will change but the criterion for determining the values for the "transition" points was not established. Proposed mechanical model does not require any "transition" point and it is applicable for any metallic layer-substrate material combination ($\alpha < 2.5$). The mechanical model is able to predict the contact radius for any layer thickness ($0 \leq t < \infty$).

The following assumptions further simplify the analysis: contacting surfaces are clean, free of oxides, the geometry of the contact area is circular, the layer is always less rigid than the indenter and the substrate, the contacting surfaces are assumed to be frictionless, the substrate is assumed to be a half-space, the contact radius must be small compared with the radius of curvature of the indenter, the contacting bodies are assumed to deform elastically, the layer, substrate and indenter materials are assumed to be isotropic.

MECHANICAL PROBLEM AND MODEL

The mechanical problem is a complex elasticity problem in an axisymmetric domain governed by the following differential equation [3]:

$$\nabla^2 \nabla^2 \phi = 0 \tag{3}$$

where ϕ is the stress function and ∇^2 is the Laplacian operator in circular coordinates. The boundary conditions are of the mixed type, with the surface deflection prescribed within the contact area and the normal stress prescribed outside. For layered bodies it is not possible to obtain a closed form solution of Eq. (3). Instead, an iterative procedure must be used based on an initial estimate of the contact radius that is then updated until the calculated normal load equals the given load within some relative error criterion.

Since there is no analytical solution to this problem, the developed model is an approximate mechanical model based on the numerical results of the model of Chen and Engel [4]. The reason for using the numerical results of the model of [4] is, that this model is the most complete model found in the open literature, which allows the contacting bodies to have elastic properties. Using the mechanical model of [4] it is possible to compute the radius of contact for any layer/substrate material combination numerically. The model assumes each body in the contact to deform elastically but computation of the contact radius requires an iterative procedure that involves the evaluation of many double integrals, consisting of special functions, using Gaussian quadrature.

The objectives of the work are: to develop a mechanical model to predict accurately the radius of contact between the hemisphere and the layered substrate for any layer material, to present a mechanical model in simple analytical form and to verify the analytical predictions by experiment and existing data.

CONTACT RADIUS BOUNDS

A computer program based on the model of [4], following [1], is written in $MATLAB\,5$ [5] to solve for the radius of contact. Several material combinations will be investigated. These material combinations are: lead/stainless steel, silver/nickel, lead/molybdenum, gold/copper and silicone rubber/stainless steel. For all cases the indenter is selected to be stainless steel. The other contact parameters such as: the layer thickness, the radius of curvature of the indenter and applied load will vary as well. The selected material mechanical and thermal properties are listed in Table 1:

Table 1. Physical Properties of Materials

Material	E GPa	ν	k W/mK
Ni 200	204	0.33	79.3
Silver	75	0.33	427
Lead	37	0.33	35.3
SS 304	207	0.33	18.4
Molybdenum	325	0.33	138
Copper	140	0.33	400
Gold	78.5	0.33	317

Once the numerical values have been computed they have to be presented in graphical form, which will allow further investigation. To simplify further analysis the bounds of the contact radius will be defined first. Also, the importance of the ratio of bounding radii will be investigated and discussed.

Figure 3a and Fig. 3c show the contact between the hemispherical indenter and a bare flat. For this type of contact, the general contact elastic solution of Hertz [3] can be used to obtain the contact radius. Because the contact occurs between the two contacting bodies, according to the Hertz theory the contact radius is a function of the applied load F, the radius of curvature ρ of the indenter and the flat and the reduced elastic modulus E^*.

If the half-space is composed of an elastic layer bonded to an elastic substrate, as shown in Fig. 3b, the Hertz theory cannot predict the actual radius of contact because the contact radius in that case is also a function of the layer thickness and the layer material properties. However, the Hertz theory will be used to calculate the minimum and maximum bounds of the contact radius.

From Fig. 3a or Fig. 3c, it can be seen that as the layer thickness t approaches zero or infinity, the layered half-space problem reduces to the Hertzian contact of an elastic half-space composed entirely of substrate material (substrate bound), or an elastic half-space composed entirely of the layer material (layer bound). The contact radii a_S and a_L for those limits are:

$$a_S = \left(\frac{3F\rho}{4E_S^*}\right)^{\frac{1}{3}} \quad \text{and} \quad a_L = \left(\frac{3F\rho}{4E_L^*}\right)^{\frac{1}{3}} \tag{4}$$

where the reduced elastic modulus for the substrate and layer is defined as:

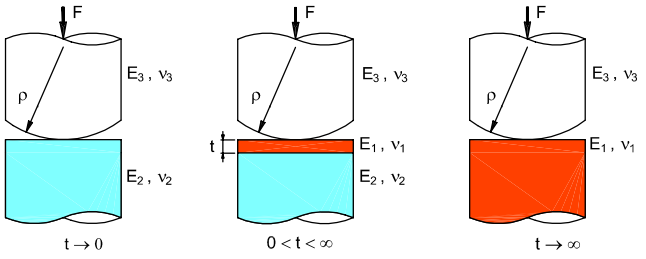

Fig.3 Contact Between Hemisphere and Layered Substrate

$$\frac{1}{E_S^*} = \frac{1-\nu_2^2}{E_2} + \frac{1-\nu_3^2}{E_3}, \quad \frac{1}{E_L^*} = \frac{1-\nu_1^2}{E_1} + \frac{1-\nu_3^2}{E_3} \tag{5}$$

For all other values of the layer thickness the radius of contact will lie between the two bounding radii, Fig. 3b:

$$a_S \le a \le a_L \tag{6}$$

MECHANICAL MODEL DEVELOPMENT

The unknown contact radius for the layered flats indented by the hemisphere is a function of nine independent variables:

$$a = f\,(t, F, \rho, E_i, \nu_i) \qquad i = 1, 2, 3 \tag{7}$$

To analyze this contact it is necessary to reduce the number of independent variables by defining new variables as function of two or more independent variables. The first step is to define the dimensionless layer thickness τ and the ratio of bounding radii α as follows:

$$\tau = \frac{t}{a} \quad \text{and} \quad \alpha = \frac{a_L}{a_S} \tag{8}$$

Then, it is necessary to define the dimensionless contact radius. A similar problem was investigated by McCormick [6], Matthewson [7] and Jaffar [8]. They introduced the dimensionless contact radius as the ratio of the contact radius a and bounding radius corresponding to the layer bound a_L.

The dimensionless contact radius a_L^* defined as a/a_L was their only choice because they assumed that the substrate and the indenter were rigid compared to the layer, which means that the bounding radius corresponding to the substrate bound is always equal to zero ($a_S = 0$). While this approach is appropriate in the case where E_2 and E_3 are much larger than E_1, it would be just a special case of the general case. By defining the α, τ and a_L^* the number of independent variables is reduced to three.

In this work it is assumed that the layer, substrate and indenter are elastic. Following the approach of the previous researchers the dimensionless contact radius can be defined either as a/a_L or a/a_S, but in both cases the dimensionless radius will be a function of just one bounding radius instead of two. In order to develop the general mechanical model for any material combination, dimensionless contact radius has to be a function of a_S as well as a_L. Also the authors would like to define a^* such the radius bounds are fixed for any material combination. This is possible simply by defining a^* as:

$$a^* = \frac{a - a_S}{a_L - a_S} \tag{9}$$

From Eq. (9) it can be seen that for the thick layers the unknown contact radius is equal to a_L and a^* is equal to one. When the layer thickness is equal to zero the contact radius is equal to a_S and a^* is equal to zero. For all other values of the layer thickness the dimensionless radius of contact a^* will lie between the two dimensionless bounding radii:

$$0 \le a^* \le 1 \tag{10}$$

By substituting Eq. (4) into Eq. (8) the ratio of bounding radii α becomes:

$$\alpha = \frac{a_L}{a_S} = \left(\frac{E_S^*}{E_L^*}\right)^{\frac{1}{3}} \tag{11}$$

For any material combination α is only a function of the cube root of the reduced elastic moduli ratio. Obviously α is not a function of applied load and the radius of curvature of the indenter. The value of α can vary from unity, for the combination where the layer and the substrate are composed of the same material, to the some very large value, for the combination where the Young's modulus of elasticity of the substrate and the indenter is much larger than that of the layer.

Table 2 gives values of α, E_S^*/E_L^* and E_L/E_S for material combinations considered in this work.

Table 2. Values of α for Different Material Combinations

Material Combination	α	E_S^*/E_L^*	E_L/E_S
Lead/Molybdenum	2.04	8.45	20.30
Lead/ SS 304	1.45	3.07	5.59
Silver/Nickel	1.23	1.86	2.72
Gold/Copper	1.14	1.47	1.78

It was found that for any metal to metal combination the value of α lies in the range:

$$1 \le \alpha \le 2.5 \tag{12}$$

The value of α can be less than unity, but because of the basic assumption that the layer is always less rigid than the substrate this case will not be considered. As the value of α increases the difference between E_L and E_S becomes larger. For example for $\alpha = 2.5$, the difference between E_L and E_S is: $E_L/E_S \approx 40$. In that case it can be assumed that the indenter and the substrate are rigid compared to the layer. Stevanović and Yovanovich [9] developed a procedure for computing the unknown radius of contact for the case where $\alpha > 2.5$.

Solutions were obtained for four material combinations. These material combinations are lead/stainless steel, silver/nickel, lead/molybdenum and gold/copper. As can be seen, these combinations are sufficient to describe a practical range of material combinations spanning the range of the ratio of bounding radii given by $0 < \alpha < 2.5$.

By plotting the dimensionless contact radius a^* versus dimensionless layer thickness τ a family of curves, each corresponding to a different value of α would be obtained. Examination of those curves does not allow immediate interpolation to material combinations that have not been considered in this work. This is due to the normalization of the nondimensional thickness with respect to the contact radius. To collapse all curves into a single curve it is necessary to introduce a new dimensionless thickness as a function of τ as well as α.

The layer thickness was nondimensionalized as:

$$\tau^* = \left(\frac{t}{a}\sqrt{\alpha}\right)^{\frac{1}{3}} \tag{13}$$

Through the use of τ^* all of the solutions collapse to essentially a single curve. The numerical results of a^* plotted as a function of τ^* are presented in Fig. 4.

The exponential function was chosen as a result of the close similarity of the numerical results to this function. It was found that the correlation equation:

$$a^* = 1 - \exp\left(-\pi^{1/4}\left(\tau\sqrt{\alpha}\right)^{\pi/4}\right) \tag{14}$$

suitably describes the numerical data through all ranges of layer thickness.

Since the unknown contact radius a appears on both sides, equation requires an iterative method to find its root. The Newton-Raphson method can be used to obtain the root. The first guess for the interative procedure is based on the average

$$\bar{a} = \frac{a_S + a_L}{2}$$

After one iteration the radius converges to five digit accuracy. The solution is presented in the following form:

$$a = a_S + (a_L - a_S)\left(1 - \exp\left(-\pi^{1/4}\left(\frac{t\sqrt{\alpha}}{a_0}\right)^{\pi/4}\right)\right) \tag{15}$$

where a_0 is defined as:

$$a_0 = a_S + (a_L - a_S)\left(1 - \exp\left(-\pi^{1/4}\left(\frac{t\sqrt{\alpha}}{\bar{a}}\right)^{\pi/4}\right)\right) \tag{16}$$

Equation (15) is the first existing closed form solution for the unknown contact radius. The maximum difference between the correlation and the model of [4] is always less than 1% for any value of τ.

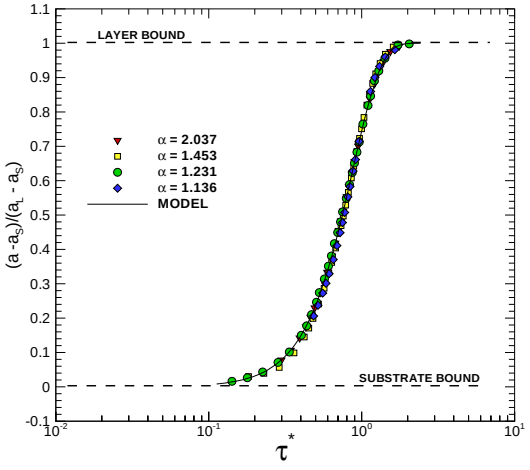

Fig. 4 a^* vs. τ^*

EXPERIMENT

To verify the model analytical predictions the thermal contact resistance measurements were performed for the bare flat. Also, the model is compared with the experimental data of [1] for the silver-nickel combination. The main reason for performing the thermal contact resistance measurements on a bare flat is to verify the zero layer thickness case, which is the upper bound on the contact resistance for the layered flat. Detailed descriptions of the test column and experimental procedure are given by Stevanović [10].

The value of the experimental contact resistance (R_{exp}) is calculated as the temperature drop at the contact (ΔT_j) divided by the heat flow rate at the contact:

$$R_{exp} = \frac{\Delta T_j}{\left(Q_{upper} + Q_{lower}\right)/2} \tag{17}$$

The temperature drop at the contact (ΔT_j) was computed as the difference in the extrapolated surface temperatures of the hemispherical indenter (T_{e2}) and test specimen (T_{e1}):

$$\Delta T_j = T_{e2} - T_{e1} \tag{18}$$

and Q_{upper} and Q_{lower} are heat flow rates through the upper and lower heat flux meters.

Bare Flats

For this series of tests a $38.1\,mm$ carbon steel hemispherical indenter and an Armco iron substrate were used as the specimens. Thermo-mechanical properties for the substrate and indenter are: $E_2 = 204\,GPa$, $k_2 = 72.4\,W/mK$, $\nu_2 = 0.3$, $E_3 = 207\,GPa$, $k_3 = 43.3\,W/mK$, $\nu_3 = 0.292$. The thermal contact resistance measurements are summarized in Table 3 and plotted versus applied load in Fig. 5. Table 3 also summarizes the thermal contact resistance theoretical values assuming pure elastic contact, elastic-plastic and pure plastic contact.

The percentage difference is defined as the relative difference between the experimental and theoretical resistance

Table 3. Comparison of Experimental Results and Theory for Bare Flat

Load (N)	R_{exp} (K/W)	R_{ep} (K/W)	$R_{elastic}$ (K/W)	$R_{plastic}$ (K/W)	$\%\, diff.$ $exp-ep$	$\%\, diff.$ $exp-elastic$	$\%\, diff.$ $exp-plastic$
25.0	44.3	49.1	49.4	104.2	-9.8	-10.3	-57.5
62.4	33.9	35.7	36.0	65.4	-4.9	-5.9	-48.2
145.7	26.1	26.1	26.7	42.1	0.0	-2.2	-38.0
157.8	24.2	25.3	25.9	40.3	-4.3	-6.6	-40.0
263.0	20.4	20.8	21.6	30.8	-2.0	-5.4	-33.8
301.0	19.7	19.8	20.6	28.8	-0.5	-4.2	-31.5
344.9	19.1	18.8	19.6	26.8	1.7	-2.6	-28.7
396.8	18.1	17.8	18.7	24.9	1.7	-3.0	-27.3

computed as follows:

$$\%\, diff. = \frac{R_{exp} - R_{theory}}{R_{theory}} \times 100\,\% \tag{19}$$

At the start of the experimental measurements it was initially assumed that the contact between contacting bodies is pure elastic, so the contact radius used to calculate the theoretical resistance was found using the Hertzian theory. The theoretical curve for pure elastic contact is shown as a dashed line in Fig. 5.

Agreement between the experimental resistance and theoretical resistance, based on the Hertzian theory, is relatively good with a maximum difference of 10.3%, but as can be seen the Hertzian theory always over predicts the measured resistance. This is because the contact is not pure elastic but rather elastic-plastic.

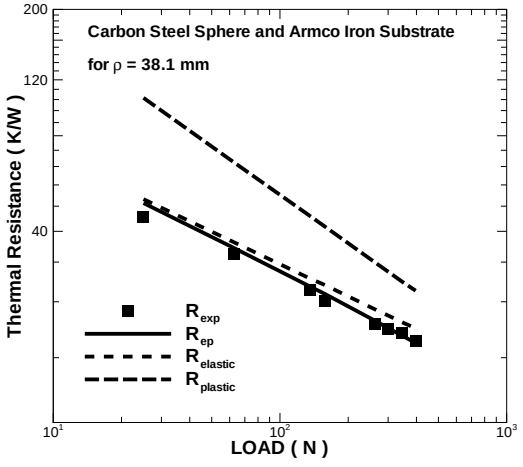

Fig. 5 Thermal Resistance vs. Applied Load

To verify this assumption the range of elastic and plastic behavior as a function of critical load F_c needs to be examined. The critical load is the load for which the elastic and the plastic theories predict the same value for the contact radius. The critical load F_c is a function of material properties and the contact geometry.

Archard [11] developed a simple technique for predicting the load range for elastic, elastic-plastic and plastic contact as a function of the critical load defined as:

$$F_c = \frac{9\,\pi^3}{16}\, H^3 \left(\frac{\rho}{E^*}\right)^2 \tag{20}$$

Three load ranges are:

Pure elastic: $F \le \frac{1}{15}\, F_c$

Elastic-plastic: $\frac{1}{15}\, F_c < F < 15\, F_c$

Pure plastic: $F \ge 15\, F_c$

For the performed tests the value of hardness is $H = 103\ kg/mm^2$. The calculated critical load is $F_c = 2030N$; the elastic-plastic transition load range begins at $F = 1/15F_c = 135N$ and ends at $F = 15F_c = 30.4kN$. The load range used in this experiment is from $25N$ to $400N$. Obviously for loads greater than $135N$ the effect of plastic deformation cannot be neglected and must be included in the theoretical contact resistance predictions.

The radius of contact within the elastic-plastic load range can be calculated using the Churchill and Usagi [12] suggestion to blend asymptotic solution for pure elastic (using Hertzian theory) and pure plastic behavior:

$$a_{ep} = \left[a_e^n + a_p^n\right]^{1/n} \tag{21}$$

where $n = 5$ is a blending parameter. This value of n is chosen because for $n = 5$ the transition begins at approximately $F = 1/15F_c = 135\,N$ and ends at approximately $F = 15F_c = 30.4\,kN$ as is shown in Fig. 6.

Contact radius for pure plastic contact is calculated as follows [1]:

$$a_p = \left[\frac{F}{\pi\, H}\right]^{1/2} \tag{22}$$

Agreement between the experimental resistance and theoretical resistance based on the elastic-plastic correction, shown as a thick continuous line in Fig. 6, is much better than for the case when we assume the pure elastic contact. Except for the first data point (-9.8%) the difference is always less than 5%. Obviously the correction for the elastic-plastic behavior gives much better results.

Layered Flats

Fisher [1] performed thermal contact resistance measurements for a silver layer on a nickel substrate for different layer thicknesses. A series of three tests were performed for the layer thicknesses of 60, 110 and 900 μm, and an applied load range from $23.9N$ to $688N$.

For each test two curves representing theoretical predictions of [1] and proposed model predictions are plotted along with the experimental thermal resistance data.

Experimental Results for $t = 60\,\mu m$. For this test series the results are plotted versus applied load in Fig. 7; the agreement with the experimental data is good. For this test series the proposed model shows better agreement with experimental data than the model of [1]. Except for the first experimental point the experimental resistance is always lower than the theoretical values. For the next six experimental points the difference is less than 10 %.

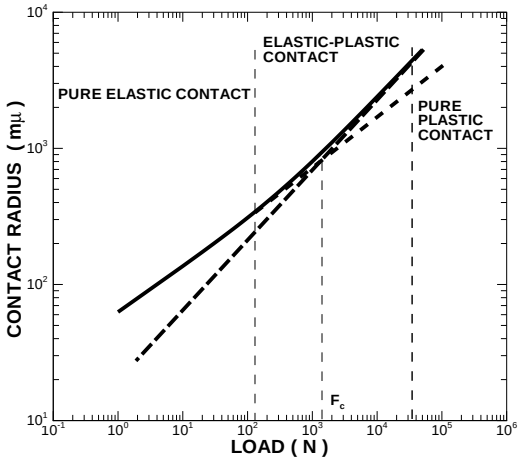

Fig. 6 Contact Radius vs. Applied Load

At higher loads the difference increases to the maximum of 20.7 %. The reasons for this behavior are the same as for the bare flat. The critical load for nickel is 2050 N and the elastic-plastic transition load range begins at 135 N.

From Fig. 7 it can be seen that for loads lower than 135 N the experimental data are in good agreement with the theoretical predictions, accept for the first data.

As the load increases the slope of the experimental data is becoming steeper because the contact behavior is elastic-plastic due to the plastic yielding of the nickel substrate.

Experimental Results for $t = 110\,\mu m$. Test results are plotted versus applied load in Fig. 8. For light loads the theoretical resistance is 20 % lower then the experimental resistance. This difference is consistent indicating a bias error rather then random error. Similarly in the previous section it can be see from Fig. 8, that for loads greater than 135 N elastic-plastic behavior occurs and the experimental data are changing slope.

Experimental Results for $t = 900\,\mu m$. Results are plotted versus applied load in Fig. 9. In this test series the experimental data are in excellent agreement with the proposed model predictions as well as with the model predictions of [1] over the full range of applied load. The proposed model shows slightly better agreement than model predictions of [1]. The measured resistance is always greater then the model predictions. The maximum difference is 10.5 % at 120 N. The data do not show the elastic-plastic behavior observed in the other tests because the silver layer is relatively thick proving that the elastic-plastic behavior observed in previous sections is related to the nickel substrate.

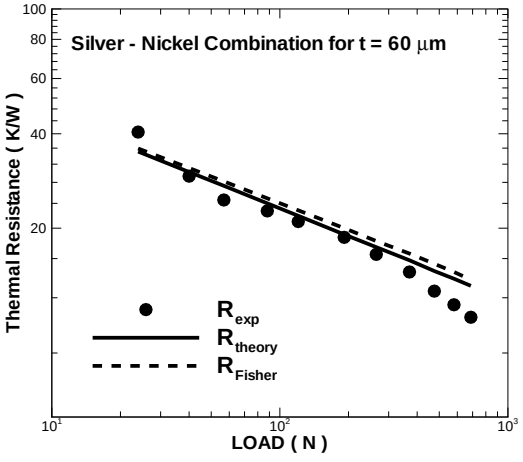

Fig. 7 Experimental Results for $t = 60\,\mu m$

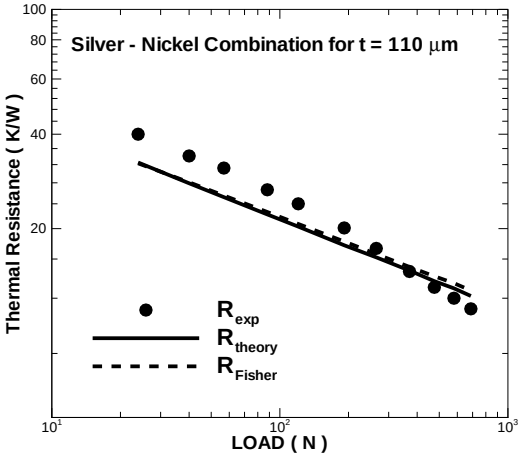

Fig. 8 Experimental Results for $t = 110\,\mu m$

Good agreement is observed between the experimental results and theoretical predictions for light loads. Comparisons with the approximate model of [1] shows that the proposed model has slightly better agreement with the experimental values, for a given material combination. For higher loads the proposed model always overpredicts the measured resistance due to plastic deformation in the nickel substrate.

Archard's elastic-plastic correction can not be applied directly, for the layered flats, because the layer and substrate have different hardness. Because the contact radius is a function of layer thickness and the ratio of the bounding radii, α, it would be necessary to make Archard's corrections for the bounding radii (a_S and a_L) first and then using the "corrected" a_S and a_L simply applying the proposed mechanical model to find the corresponding contact radius.

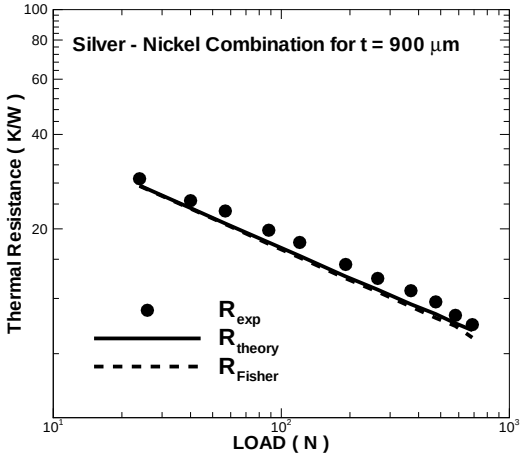

Fig. 9 Experimental Results for $t = 900\,\mu m$

There is another possible way to make necessary corrections for the elastic-plastic behavior. To apply Archard's technique the effective hardness of the layer/substrate combination can be used to predict the contact radius for pure plastic contact, a_p. Antonetti and Yovanovich [13] demonstrated the method for computing the effective hardness for layered substrates. By substituting the "corrected" value for a_p in Eq. (21) the radius of contact corrected for elastic-plastic behavior can be found.

SUMMARY AND CONCLUSIONS

An approximate model for finding the contact radius of an elastic hemispherical indenter in contact with an elastic layer on an elastic substrate is presented in the form of a close-form equation for the unknown radius of contact.

The proposed mechanical model does not require any "transition" point and it is applicable for any metallic layer-substrate material combination ($\alpha < 2.5$). The mechanical model can be used to predict the contact radius for any layer thickness ($0 \leq t \leq \infty$).

The agreement between the experimental data and theoretical predictions is very good for light loads within the elastic load range. At the higher loads the theory overpredicts the measured thermal resistance due to plastic deformation of the substrate. With the theoretical predictions corrected for elastic-plastic contact behavior excellent agreement between theoretical predictions and experimental measurements is obtained for the full load range. Future work is recommended to verify experimentally the model predictions for other layer-substrate combinations.

ACKNOWLEDGMENTS

The first author acknowledges the financial support of C-MAC Engineering Inc. The other authors acknowledge the continued financial support of the Natural Sciences and Engineering Research Council.

REFERENCES

[1] Fisher, N.J., "Analytical and Experimental Studies of the Thermal Contact Resistance of Sphere/Layered Flat", M.A.Sc. Thesis, 1985, University of Waterloo, Canada

[2] Dryden, J.R., "The Effect of a Surface Coating on the Constriction Resistance of a Spot on an Infinite Half Plane," *J. Heat Transfer*, Vol. 105, No. 2, May 1983, pp. 408-410.

[3] Timoshenko, S. and Goodier, J.N., *Theory of Elasticity*, 2nd Edition, McGraw-Hill, New York, 1951.

[4] Chen, W.T. and Engel, P.A., "Impact and Contact Stress Analysis in Multilayer Media," *Int. J. Solids Structures*, Vol. 8, 1972, pp. 1257-1281.

[5] Matlab Version 5 , *The MathWorks, Inc.*

[6] McCormick, J.A., "Numerical Solutions for General Elliptical Contact of Layered Elastic Solids," MTI Report No. 78TR52, 1978, Mechanical Technology, Latham, New York.

[7] Matthewson, M.J.,"Axi-Symmetric Contact on Thin Compliant Coatings," *J. Mech. Phys. Solids*, Vol. 29, 1981, No. 2, pp. 89-113.

[8] Jaffar, M.J., "A Numerical Solution for Axisymmetric Contact Problems Involving Rigid Indenters on Elastic Layers," *J. Mech. Phys. Solids*, Vol. 36, 1988, No. 4, pp. 401-416.

[9] Stevanović, M. and Yovanovich, M.M., "Modeling Thermal Constriction Resistance of Sphere-Layered Substrate in Elastic Contact," AIAA 99-1049, 37^{th} AIAA Aerospace Science Meeting and Exhibit, January 1999, Reno, Nevada

[10] Stevanović, M., "Modeling Thermal Constriction Resistance of Hemisphere-Layered Substrate in Elastic Contact", M.A.Sc. Thesis, 2001, University of Waterloo, Waterloo, Canada

[11] Archard, J.F., "Wear Theory and Mechanisms", *Wear Control Handbook*, edited by M.B. Peterson and W.O. Winer, ASME, New York, 1980, pp.35-80.

[12] Churchill, S.W., and Usagi, R., A General Expression for the Correlation of Rates of Transfer and Other Phenomena, *AIChE J.*, Vol. 18, No. 6, pp. 1121-1138, 1972.

[13] Antonetti, V.W. and Yovanovich, M.M., "Enhancement of Thermal Contact Conductance by Metallic Coatings: Theory and Experiment", *J. Heat Transfer*, Vol. 107, August 1985, pp. 513-519.